Preliminary experience with superparamagnetic iron oxide-enhanced dynamic magnetic resonance imaging and comparison with contrast-enhanced computed tomography in endoleak detection after endovascular aneurysm repair

Shigeo Ichihashi, MD,[a] Nagaaki Marugami, MD,[a] Toshihiro Tanaka, MD,[a] Shinichi Iwakoshi, MD,[a] Norio Kurumatani, MD,[b] Satoru Kitano, MD,[a] Akihiro Nogi, RT,[a] and **Kimihiko Kichikawa, MD,[a]**
Nara, Japan

Objective: **Contrast-enhanced computed tomography (CE-CT) has been commonly used for follow-up imaging after endovascular aneurysm repair (EVAR), but it is difficult to use on patients with renal insufficiency. Superparamagnetic iron oxide (SPIO) particles, contrast medium for magnetic resonance imaging (MRI) that has been widely used for detection of the liver tumor, rarely affects renal function. The present study examined SPIO-enhanced dynamic MRI as a potential alternative to CE-CT for detection of endoleaks after EVAR.**
Methods: **Institutional review board approval was obtained for this prospective study. Twenty-three consecutive patients with normal renal function were evaluated using both CE-CT and SPIO-enhanced MRI within 2 weeks after EVAR. The median interval between the two modalities was 2 days. SPIO-enhanced MRI was performed at 1.5 T with T1-weighted, SPIO-enhanced dynamic, and postcontrast T1-weighted gradient echo sequences. The CE-CT protocol consisted of triple scans. Two experienced, blinded observers evaluated all images. Consensus reading of CE-CT and SPIO-MRI was defined as the reference standard. Interobserver, intraobserver, and intermodality agreement for endoleak detection was assessed by κ statistics.**
Results: **A total of 11 type II endoleaks originating from either the lumbar or inferior mesenteric artery were detected. Eight were able to be detected by CE-CT (8/11:73%) and 10 (10/11:91%) by SPIO-enhanced MRI. Interobserver (κ = 0.91; 95% CI, 0.74-1.00) and intraobserver agreement for MRI (κ = 1.00) were excellent. Intermodality agreement for endoleak detection was moderate (κ = 0.63; 95% CI, 0.32-0.94; and κ = 0.62; 95% CI, 0.29-0.95 for observers A and B, respectively).**
Conclusions: **SPIO-enhanced MRI could represent a useful alternative to CE-CT, as it offers excellent interobserver, intraobserver agreement, and could detect more endoleaks than CE-CT. (J Vasc Surg 2013;58:66-72.)**

During the last decade, endovascular aneurysm repair (EVAR) has become the important modality of treatment for abdominal aortic aneurysms (AAA). Although previous multiple randomized controlled trials showed lower 30-day mortality with EVAR, compared with open AAA repair, the procedure has also been associated with postoperative complications such as endoleaks, and a significantly higher rate of secondary interventions.[1,2] Because endoleaks may cause enlargement of aneurysm sac and, thus, increase the risk of rupture after EVAR, long-term surveillance of endoleaks is necessary to allow for secondary interventions to maintain optimal outcomes.[3]

Contrast-enhanced computed tomography (CE-CT) has been commonly used for postoperative surveillance of EVAR because, in part, of its rapid acquisition time and high diagnostic value. However, it is also associated with the cumulative risks of radiation exposure and, most of all, contrast nephrotoxicity. With increasing reliance on diagnostic CT using iodinated intravenous contrast, the incidence of contrast-induced nephropathy is likely to increase. In a previous article evaluating contrast-induced nephropathy after percutaneous coronary intervention, more severe renal impairment was found to be correlated with a greater risk of developing contrast-induced nephropathy,[4] so that the risk is highest in patients with chronic kidney disease (CKD).

Dynamic contrast-enhanced magnetic resonance imaging (MRI) techniques using gadolinium diethylenetriamine penta-acetic acid (Gd-DTPA) as a contrast agent have been shown to be very sensitive for depicting small endoleaks[5] and can have additional value for their classification.[6] However, the association between nephrogenic

From the Department of Radiology[a] and Department of Community Health and Epidemiology,[b] Nara Medical University.
Author conflict of interest: none.
Reprint requests: Shigeo Ichihashi, MD, Department of Radiology, Nara Medical University, 840 Shijo-cho, Kashihara, Nara 634-8521, Japan (e-mail: shigeoichihashi@yahoo.co.jp).
The editors and reviewers of this article have no relevant financial relationships to disclose per the JVS policy that requires reviewers to decline review of any manuscript for which they may have a conflict of interest.
0741-5214/$36.00

http://dx.doi.org/10.1016/j.jvs.2012.12.061

systemic fibrosis and gadolinium-based contrast agents has been reported in patients with CKD.[7,8] Contrast-enhanced ultrasound (CE-US) has also been shown to be sensitive for detecting endoleaks and to allow for better classification of endoleaks compared with CE-CT.[9] However, diagnostic accuracy of CE-US depends largely on operator skill, and scan and study qualities are generally poor in obese patients.

Superparamagnetic iron oxide (SPIO) particles were originally developed as contrast medium for MRI of the liver, where they are administered to improve tumor detection with T2-weighted imaging (T2WI). The SPIO particles improve contrast by being taken up by the Kupffer cells of normal liver tissues but not by metastases or primary liver tumors. Intravenously injected SPIO particles also shorten the T1 relaxation time, and thus, vascularized structures show signal enhancement on T1-weighted imaging (T1WI),[10,11] so SPIO-enhanced MRI may have the potential to detect endoleaks. SPIO is different from Gd-DTPA. SPIO is metabolized as iron, the rate of urinary excretion is less than 0.5%, and it is extremely rare that SPIO complicates renal function.[12,13] If SPIO-enhanced MRI is proven to be effective for endoleak detection, it should be useful for monitoring patients with CKD after EVAR. The purpose of this study was to examine SPIO-enhanced MRI as a potential alternative to CE-CT for detection of endoleaks after EVAR.

METHODS

Patients. Twenty-three consecutive patients who underwent implantation of nitinol aortic stent grafts for AAA were recruited to this prospective study. No patients had contraindications of use of SPIO (ie, history of iron allergy or hemochromatosis), and administration of SPIO could be performed in every patient. The median patient age was 79 (range, 71-83) years (male, n = 20; female, n = 3). The median body weight was 61 kg (range, 45-71 kg). The median sac diameter was 48.5 mm (range, 44.5-53.7 mm). Excluder stent grafts (Gore Medical, Newark, Del) were implanted in 10 patients and Endurant stent grafts (Medtronic, Fridley, Minn) were implanted in 13. CE-CT and SPIO-enhanced MRI were performed for endoleak detection within 2 weeks after EVAR. The time period between CE-CT and SPIO-enhanced MRA was not more than 1 week. Written informed consent was obtained from all patients. The institutional review board approved this prospective study.

CE-CT. All examinations were performed with a dual-source 64 slice CT scanner (Somatom Definition; Siemens Medical Solutions, Erlangen, Germany). A triple-phase CT protocol consisting of a nonenhanced, arterial and a delayed venous phase encompassing the abdomen and pelvis from the level of the cardiac apex to the femoral head was performed. After standard nonenhanced data acquisition, arterial phase scanning was performed using a bolus-tracking technique. A total of 100-150 mL of nonionic iodinated contrast medium was administered at a flow rate of 4 mL/s. All injections were followed by a chaser bolus of 30 mL of saline solution. The arterial phase data acquisition was initiated 6 seconds after the attenuation reached a predefined threshold of 120 HU. This delay allowed the patient to receive breathing instructions and facilitated maximal aortic enhancement. Delayed phase dual-energy CT scanning was performed with a standard delay of 70 seconds after the beginning of the contrast material injection.

SPIO-enhanced MRI. All scans were performed at 1.5 T (Siemens Medical Solutions). Before injection of SPIO, native turbo fast low angle shot magnetic resonance imaging (FLASH) and volumetric interpolated breath-hold examination (VIBE) sequences were performed under breath-hold conditions (Table I). Resovist (Fujifilm RI Pharma Co, Tokyo, Japan), a bolus injectable SPIO, was used as the contrast medium. Depending on patient weight, a dose of 0.6-1.4 mL (0.016 mL/kg body weight) of Resovist was injected at 1.0 mL/s followed by a 20 mL saline flush administered at the same rate using an electronic power injector (Spectris Solaris; Medrad, Warrendale, Pa). After injection, the fluoroscopic triggering technique using two-dimensional sagittal gradient refocused images (CareBolus technique) was obtained rapidly through the thoracic aorta. When the contrast bolus arrived at the descending aorta, the turbo FLASH sequence was started for the vascular phase. The VIBE sequence was started 2 minutes after injection. These series were also evaluated after subtraction processing. Subtraction imaging is a technique whereby an unenhanced T1-weighted sequence is digitally subtracted from the identical sequence performed after SPIO administration. By performing this operation, the native T1 signal is removed and any signal remaining on the subtracted images is due solely to enhancement (ie, endoleaks). MR angiography (MRA) images were also obtained by maximal intensity projection processing on subtraction images.

Image analysis. Analysis of CE-CT and SPIO-enhanced MRI was performed by two independent radiologists (S.I. and N.M., with 9 and 16 years of experience in vascular imaging, respectively) who were blinded to previous angiographic results. Both readers independently reviewed all images and evaluated the presence and types of endoleaks. The order in which the different reading sessions were performed was selected randomly by another radiologist (T.T.) who was not involved in the reading sessions. The classification of endoleaks was performed according to the criteria proposed by White et al[14]: type I, II, III, IV, and unknown (meaning the exact site of inflow could not be identified). One observer (S.I.) evaluated CE-CT and SPIO-enhanced MRI twice for intraobserver comparison with an interval between the first and second evaluations of more than 1 month. During the second evaluation, the observer was blinded to the results of the first evaluation. In addition to the endoleak evaluation, patencies of the endografts and renal arteries were also evaluated by a single observer (S.I.) referring to the MRA. Dynamic scans were considered technically unsuccessful if

Table I. MRI scan parameter

Parameter	*Turbo FLASH*	*VIBE*
TR, milliseconds	2.51	2.95
TE, milliseconds	0.88	1.1
FA, °	25	10
Slice thickness, mm	1.5	3
FOV, mm	350	350
Matrix	147 × 256	176 × 256
Slice per slab	128	60
Scan time, seconds	16	25

FA, Flip angle; *FLASH,* fast low angle shot magnetic resonance imaging; *FOV,* field of view; *MRI,* magnetic resonance imaging; *TE,* echo time; *TR,* repetition time; *VIBE,* volumetric interpolated breath-hold examination.

diagnostic evaluation was seriously compromised by patient motion, fold-over artifacts, or misregistration artifacts.

Statistical analysis. Categorical variables are expressed as frequencies or percentages. Interobserver, intraobserver, and intermodality agreements for endoleak detection were assessed by κ statistics as follows: κ values of 0.00-0.40 were considered to indicate poor agreement; 0.41-0.75, fair to good agreement; and 0.76-1.00, excellent agreement.[15] When disagreements were encountered between the two readers about the existence of endoleaks, a discussion was held until consensus could be reached. Consensus reading of MRI and multidetector computed tomography studies was defined as reference standard, similar to previous studies.[5,16] All statistical tests were performed using SPSS v. 20 software (IBM, New York, NY).

RESULTS

The median interval between CE-CT and SPIO-enhanced MRI was 2 days (0-7 days). All patients completed the protocol, and no adverse events were recorded. All MRI images could be evaluated without significant motion or misregistration artifacts, and there were no unsuccessful scans.

At consensus reading, endoleaks were detected in 11 patients in total by CT and/or MRI (11/23:47%). All endoleaks were type II and originated from either the lumbar (n = 6) or inferior mesenteric artery (n = 5). CE-CT was able to detect eight of the endoleaks (8/11:73%) and SPIO-enhanced MRI was able to detect 10 (10/11:91%) (Table II; Fig 1). All 10 endoleaks detected by SPIO-enhanced MRI were detected by subtraction dynamic images, whereas three endoleaks were not detected by nonsubtraction conventional dynamic images. One type II endoleak from the lumbar artery and two type II endoleaks from the inferior mesenteric artery visualized by SPIO-enhanced MRI could not be detected by CE-CT (Fig 2). These endoleaks broadened with time on dynamic scan and connected with the lumbar artery or the inferior mesenteric artery, which were thought to be origin of the endoleaks. On the other hand, one type II endoleak from the lumbar artery visualized by CE-CT could not be detected by SPIO-enhanced MRI. A consensus reading was required for one patient in both CE-CT and SPIO-enhanced MRI. Misregistration artifacts were seen in three cases, although these artifacts did not affect the image interpretations. Interobserver (κ = 0.91; 95% CI, 0.74-1.00) and intraobserver agreement for MRI (κ = 1.00) were excellent. Intermodality agreement for endoleak detection was moderate (κ = 0.63; 95% CI, 0.32-0.94; and κ = 0.62; 95% CI, 0.29-0.95 for observers A and B, respectively).

Table II. Summary of the type II endoleaks detected by CT and/or MRI

Patient number	*Age*	*Sex*	*Endograft*	*CT*	*MRI*	*Endoleak origin*
1	92	M	Excluder	+	+	LA
2	74	M	Endurant	+	+	LA
3	76	F	Excluder	+	+	LA
4	78	F	Endurant	+	+	LA
5	83	M	Endurant	+	+	IMA
6	71	M	Endurant	+	+	IMA
7	81	M	Endurant	+	+	IMA
8	65	M	Excluder	+	−	LA
9	86	F	Excluder	−	+	IMA
10	59	M	Excluder	−	+	IMA
11	72	M	Endurant	−	+	LA

CT, Computed tomography; *F,* female; *IMA,* inferior mesenteric artery; *LA,* lumbar artery, *M,* male; *MRI,* magnetic resonance imaging; +, detected; −, undetected.

Graft and renal artery patency could be evaluated in all patients (Fig 3). All renal arteries were patent; however, in one patient, after implantation of the Excluder endograft, stenosis of the ipsilateral limb because of compression by the contralateral limb was clearly detected by MRA (Fig 4). In this patient, additional kissing balloon dilation was performed as a secondary intervention.

DISCUSSION

Endoleaks are frequent problems after EVAR. Previous CE-CT-based studies have shown that 20%-40% of patients had an initial endoleak, many of which were type II.[17] In the present study, type II endoleaks were able to be detected in eight patients by CE-CT and in 10 patients by SPIO-enhanced MRI. Sensitivity of CE-CT for endoleak detection has been reported to be 82%-83%.[9,18] On the other hand, contrast-enhanced MRI using Gd-DTPA has been shown to be significantly more sensitive for endoleak detection than CE-CT because of the high sensitivity, intrinsic three dimensionality, and excellent soft tissue contrast.[5]

Resovist, the bolus injectable SPIO, shortens both T1 and T2 relaxation times, but the shortening of T2 is much greater than that of T1.[19] The positive T1 contrast effect is less pronounced compared with Gd-DTPA.[20-22] Unlike Gd-DTPA, however, Resovist is characterized by a biexponential blood half-life of 3.9-5.8 minutes and a blood pool effect.[22] Therefore, it was hypothesized that Resovist may have the potential to allow evaluation of endoleak detection after EVAR. The present study showed

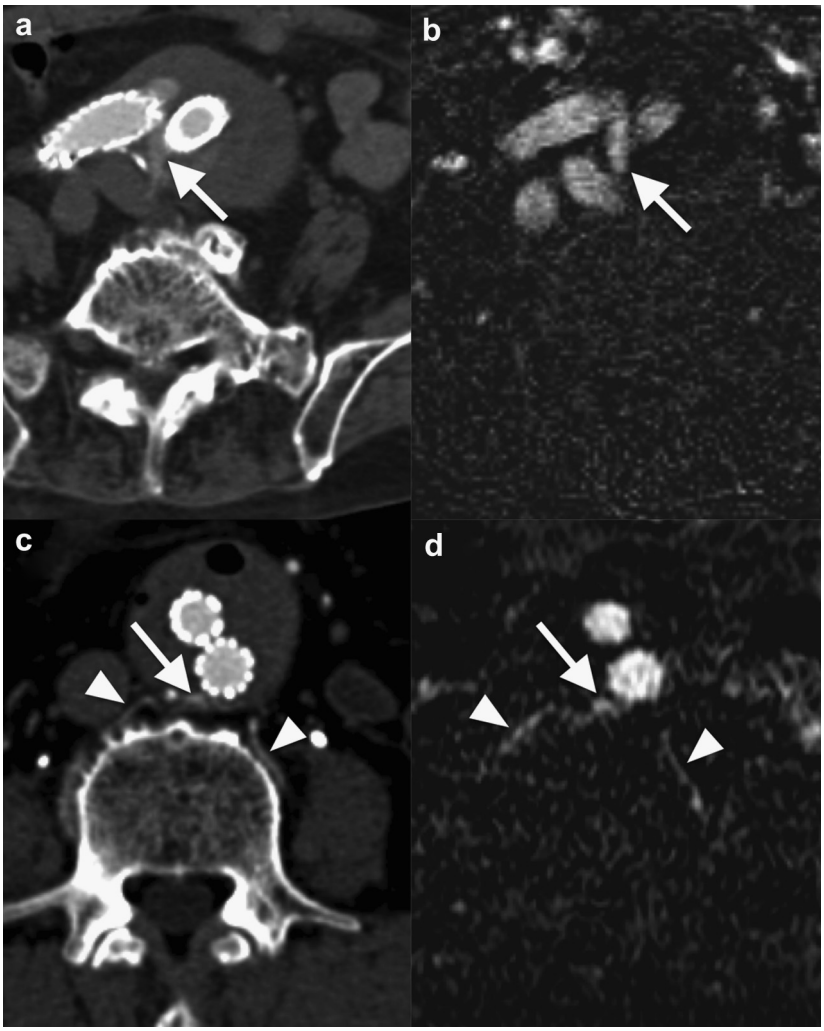

Fig 1. a, Contrast-enhanced computed tomography (CE-CT) demonstrates type II endoleak from lumbar artery. **b,** Superparamagnetic iron oxide (SPIO)-enhanced magnetic resonance imaging (MRI) also clearly demonstrates type II endoleak from lumbar artery. **c,** CE-CT in another patient demonstrates minimal type II endoleak from lumbar artery. **d,** SPIO-enhanced MRI also shows type II endoleak from lumbar artery.

that the interobserver and intraobserver agreement for MRI were excellent and the intramodality agreement between CE-CT and SPIO-enhanced MRI was fair to good. Intermodality agreement was lower than the intraobserver and interobserver agreement because the number of endoleaks detected by SPIO-MRI was greater than by CE-CT. Therefore, SPIO-enhanced MRI might be a useful alternative to CE-CT, and the ability to detect endoleaks with SPIO-enhanced MRI could be higher than in CE-CT.

Subtraction dynamic sequences under breathholding were key images for detecting endoleaks. Among the 10 endoleaks detected by subtraction dynamic sequences, only seven were detected by conventional dynamic scans. Possible reasons for this include the fact that an aneurysm sac contains fresh thrombus that shows as high intensity signal on T1WI. The minimally enhanced areas, such as type II endoleaks among the T1WI high signal clots, could be easily overlooked. Removing any pre-existing signal in T1WI unenhanced images causes contrast enhancement within an aneurysmal sac to become more conspicuous on subtracted sequences.

Misregistration artifacts are a drawback of subtraction processing.[23] An imperative technical principle of subtraction imaging is to keep all parameters constant on the unenhanced and contrast-enhanced images and to ensure that the patient's position remains unchanged. Misregistration artifacts were identified in three cases in this study, probably because of patient movement. However, these artifacts did not affect image interpretation.

This study also demonstrated that SPIO-enhanced MRI could be used for MRA, and clearly showed patency of the graft or renal arteries. Stenosis of a grafted limb was clearly demonstrated by MRA in one patient. In addition to endoleak evaluation, post-EVAR analysis such as renal

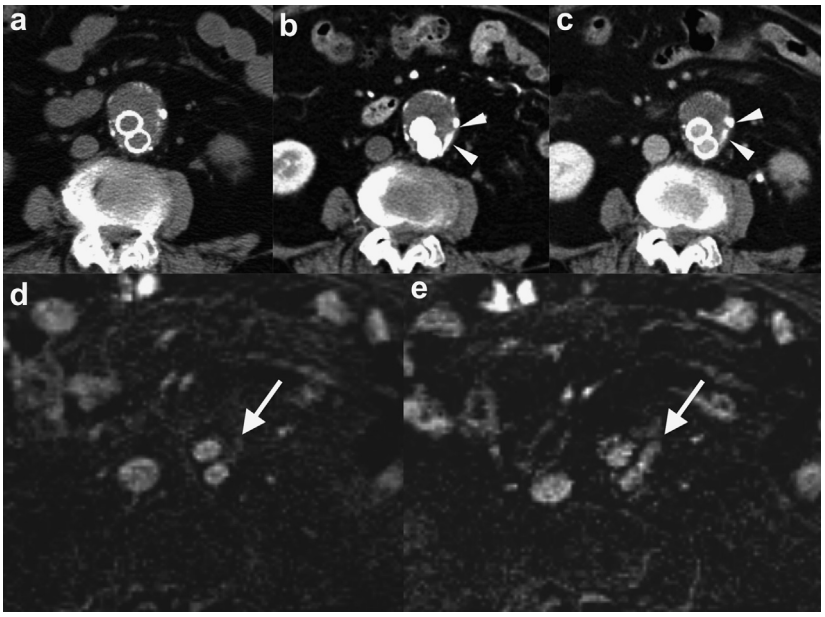

Fig 2. a, Plain computed tomography (CT). **b,** Contrast-enhanced computed tomography (CE-CT), arterial phase. **c,** CE-CT, equilibrium phase. **d,** Magnetic resonance imaging (MRI) dynamic series. **e,** Equilibrium phase, 2 minutes after superparamagnetic iron oxide (SPIO) injection. CT images shows **(a-c)** no enhanced lesion in the aneurismal sac. *Arrowheads* indicate calcifications of the arterial wall. MRI subtraction dynamic image **(d** and **e)** shows enhanced lesion in the left side of the graft and the enhanced area broadened on equilibrium phase.

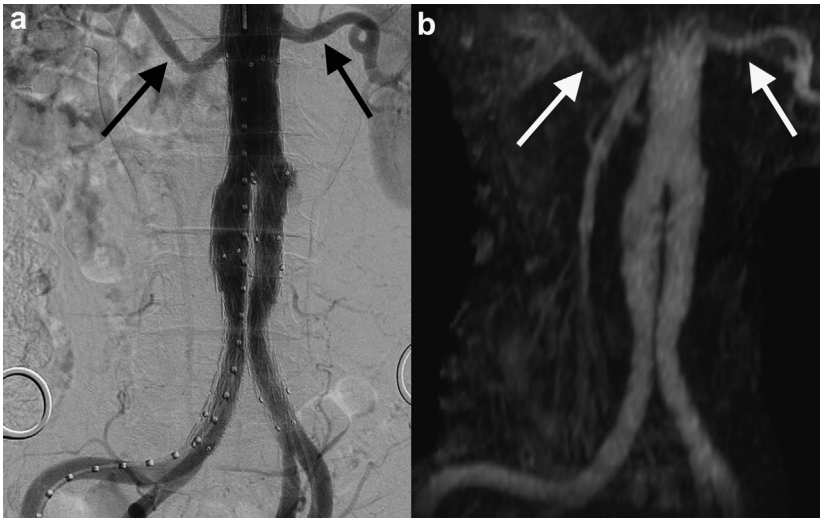

Fig 3. a, Completion angiogram after endovascular aneurysm repair (EVAR) shows bilateral renal arteries (*arrows*) are patent. **b,** Superparamagnetic iron oxide (SPIO)-enhanced magnetic resonance angiography (MRA) clearly shows patent bilateral renal arteries (*arrows*) same as completion angiogram.

artery coverage or graft kinking/stenosis might be able to be evaluated by SPIO-enhanced MRI.

Contraindication of the use of SPIO is the presence of iron allergy or hemochromatosis. On the other hand, anaphylaxis, headache, back pain, and nausea have been listed as side effects of Resovist; however, this frequency has been reported to be less than 1%. SPIO particles are mostly taken up by the reticuloendothelial system in the liver and spleen and metabolized as iron. There is no risk of toxicity if SPIO is used within normal dose. No acute or subacute toxic effects were detected by histologic or serologic studies in rats or beagle dogs who received a total

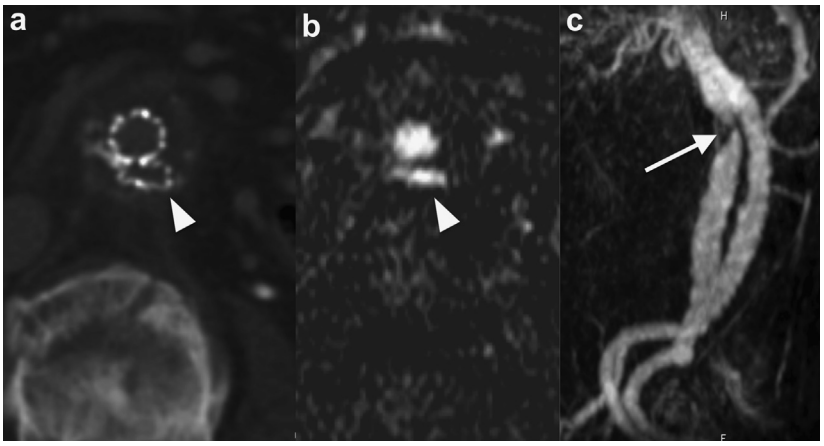

Fig 4. a, Plain computed tomography (CT) axial image. **b,** Superparamagnetic iron oxide (SPIO)-enhanced dynamic magnetic resonance imaging (MRI) axial image with subtraction. **c,** Magnetic resonance angiography (MRA). **a** and **b,** *Arrowheads* show compression of the left iliac limb. SPIO-enhanced MRA **(c)** clearly showed the stenosis of the left iliac limb (*arrow*).

of 3000 tmol Fe/kg, 150 times the dose proposed for MR imaging of the liver.[12]

The most significant advantage of using SPIO-enhanced MRI is that SPIO is free of adverse effects on renal function and can be used in patients with CKD. CE-US may be available in CKD patients; however, its diagnostic accuracy largely depends on operator skill, and its reproducibility is relatively low compared with SPIO-enhanced MRI, especially in obese patients. Furthermore, it is noteworthy that SPIO-enhanced MRI may visualize the thoracic cavity and, thus, be useful for post-thoracic endovascular aortic repair surveillance, although further investigation of post-thoracic endovascular aortic repair patients is necessary.

The present study has several limitations. First, this is a preliminary report, and the study population was small. Second, we used consensus reading of both observers evaluating CT and MRI data as the standard of reference similar to previous studies,[5,16] and we did not perform digital subtraction angiography or CE-US to confirm three endoleaks that were detected only by MRI; however, these endoleaks broadened with time on dynamic scan and connected with the lumbar artery or the inferior mesenteric artery, which were thought to be the origin of the endoleaks. In addition, a consensus reading was required for only one patient in SPIO-enhanced MRI. This is why it could be quite unlikely that these were false positives. Third, because ferromagnetic stainless steel stents might carry the risk of migration and extensive artifacts, only MRI-compatible nitinol stent grafts were included in this study. Fourth, in this study, SPIO-enhanced MRI was conducted only in patients without renal dysfunction. Fifth, cost of SPIO-MRI might well be more expensive than CE-CT. Finally, although ultrasmall SPIO with a longer blood half-life may be more suitable for endoleak detection,[24,25] ultrasmall SPIO was not available in our country during the study period.

In conclusion, SPIO-enhanced MRI may be a useful alternative to CE-CT for detection of endoleaks after EVAR. Large-scale studies including patients with renal impairment are mandatory to obtain conclusive evidence in support of the use of SPIO-enhanced MRI for detection of endoleaks after EVAR.

AUTHOR CONTRIBUTIONS

Conception and design: S Ichihashi, NM, SK, AN, KK
Analysis and interpretation: S Ichihashi, NM, TT, NK, KK
Data collection: NM, TT, S Iwakoshi
Writing the article: S Ichihashi, NM, TT, SK, AN
Critical revision of the article: S Ichihashi, TT, S Iwakoshi, KK
Final approval of the article: S Ichihashi, NM, TT, S Iwakoshi, NK, SK, AN, KK
Statistical analysis: S Ichihashi, NK, SK
Obtained funding: Not applicable
Overall responsibility: S Ichihashi

REFERENCES

1. Greenhalgh RM, Brown LC, Powell JT, Thompson SG, Epstein D, Sculpher MJ. Endovascular versus open repair of abdominal aortic aneurysm. N Engl J Med 2010;362:1863-71.
2. De Bruin JL, Baas AF, Buth J, Prinssen M, Verhoeven EL, Cuypers PW, et al. Long-term outcome of open or endovascular repair of abdominal aortic aneurysm. N Engl J Med 2010;362:1881-9.
3. Blum U, Voshage G, Lammer J, Beyersdorf F, Töllner D, Kretschmer G, et al. Endoluminal stent grafts for infrarenal abdominal aortic aneurysms. N Engl J Med 1997;336:13-20.
4. Rihal CS, Textor SC, Grill DE, Berger PB, Ting HH, Best PJ, et al. Incidence and prognostic importance of acute renal failure after percutaneous coronary intervention. Circulation 2002;105:2259-64.
5. van der Laan MJ, Bartels LW, Viergever MA, Blankensteijn JD. Computed tomography versus magnetic resonance imaging of endoleaks after EVAR. Eur J Vasc Endovasc Surg 2006;32:361-5.
6. van der Laan MJ, Bakker CJ, Blankensteijn JD, Bartels LW. Dynamic CE-MRA for endoleak classification after endovascular aneurysm repair. Eur J Vasc Endovasc Surg 2006;31:130-5.

7. Marckmann P, Skov L, Rossen K, Dupont A, Damholt MB, Heaf JG, et al. Nephrogenic systemic fibrosis: suspected causative role of gadodiamide used for contrast-enhanced magnetic resonance imaging. J Am Soc Nephrol 2006;17:2359-62.
8. Grobner T. Gadolinium: a specific trigger for the development of nephrogenic fibrosing dermopathy and nephrogenic systemic fibrosis? Nephrol Dial Transplant 2006;21:1104-8.
9. Cantisani V, Ricci P, Grazhdani H, Napoli A, Fanelli F, Catalano C, et al. Prospective comparative analysis of color-Doppler ultrasound, contrast-enhanced ultrasound, computed tomography and magnetic resonance in detecting endoleak after endovascular abdominal aortic aneurysm repair. Eur J Vasc Endovasc Surg 2011;41:186-92.
10. Schnorr J, Wagner S, Abramjuk C, Drees R, Schink T, Schellenberger EA, et al. Focal liver lesions: SPIO-, gadolinium-, and ferucarbotran-enhanced dynamic T1-weighted and delayed T2-weighted MR imaging in rabbits. Radiology 2006;240:90-100.
11. Saini S, Edelman RR, Sharma P, Li W, Mayo-Smith W, Slater GJ, et al. Blood-pool MR contrast material for detection and characterization of focal hepatic lesions: initial clinical experience with ultrasmall superparamagnetic iron oxide (AMI-227). AJR Am J Roentgenol 1995;164:1147-52.
12. Weissleder R, Stark DD, Engelstad BL, Bacon BR, Compton CC, White DL, et al. Superparamagnetic iron oxide: pharmacokinetics and toxicity. AJR Am J Roentgenol 1989;152:167-73.
13. Kopp AF, Laniado M, Dammann F, Stern W, Grönewäller E, Balzer T, et al. MR imaging of the liver with Resovist: safety, efficacy, and pharmacodynamic properties. Radiology 1997;204:749-56.
14. White GH, Yu W, May J, Chaufour X, Stephen MS. Endoleak as a complication of endoluminal grafting of abdominal aortic aneurysms: classification, incidence, diagnosis, and management. J Endovasc Surg 1997;4:152-68.
15. Fleiss JL. Statistical methods for rates and proportions. 2nd ed. New York: Wiley; 1981.
16. Alerci M, Oberson M, Fogliata A, Gallino A, Vock P, Wyttenbach R. Prospective, intraindividual comparison of MRI versus MDCT for endoleak detection after endovascular repair of abdominal aortic aneurysms. Eur Radiol 2009;19:1223-31.
17. Jones JE, Atkins MD, Brewster DC, Chung TK, Kwolek CJ, LaMuraglia GM, et al. Persistent type 2 endoleak after endovascular repair of abdominal aortic aneurysm is associated with adverse late outcomes. J Vasc Surg 2007;46:1-8.
18. Bargellini I, Cioni R, Napoli V, Petruzzi P, Vignali C, Cicorelli A, et al. Ultrasonographic surveillance with selective CTA after endovascular repair of abdominal aortic aneurysm. J Endovasc Ther 2009;16:93-104.
19. Wang YX. Superparamagnetic iron oxide based MRI contrast agents: current status of clinical application. Quant Imaging Med Surg 2011;1:35-40.
20. Hamm B, Staks T, Taupitz M, Maibauer R, Speidel A, Huppertz A, et al. Contrast enhanced MR imaging of liver and spleen: first experience in humans with a new superparamagnetic iron oxide. J Magn Reson Imaging 1994;4:659-68.
21. Reimer P, Rummeny EJ, Daldrup HE, Balzer T, Tombach B, Berns T, et al. Clinical results with Resovist: a phase 2 clinical trial. Radiology 1995;195:489-96.
22. Reimer P, Marx C, Rummeny EJ, Müller M, Lentschig M, Balzer T, et al. SPIO-enhanced 2D-TOF MR-angiography of the portal venous system: results of an intraindividual comparison. J Magn Reson Imaging 1997;7:945-9.
23. Newatia A, Khatri G, Friedman B, Hines J. Subtraction imaging: applications for nonvascular abdominal MRI. AJR Am J Roentgenol 2007;188:1018-25.
24. Sharma R, Saini S, Ros PR, Hahn PF, Small WC, de Lange EE, et al. Safety profile of ultrasmall superparamagnetic iron oxide ferumoxtran-10: phase II clinical trial data. J Magn Reson Imaging 1999;9:291-4.
25. Tombach B, Reimer P, Bremer C, Allkemper T, Engelhardt M, Mahler M, et al. First-pass and equilibrium-MRA of the aortoiliac region with a superparamagnetic iron oxide blood pool MR contrast agent (SH U 555 C): results of a human pilot study. NMR Biomed 2004;17:500-6.

Submitted Oct 19, 2012; accepted Dec 19, 2012.